Evolution from quasivibrational to quasirotational structure in ^{155}Tm and yrast $27/2^-$ to $25/2^-$ energy anomaly in the $A \approx 150$ mass region

L. Liu (刘雷),[1,2] S. Y. Wang (王守宇),[1,*] S. Wang (王硕),[1] H. Hua (华辉),[3] S. Q. Zhang (张双全),[3] J. Meng (孟杰),[3,†] R. A. Bark,[4] S. M. Wyngaardt,[5] B. Qi (亓斌),[1] D. P. Sun (孙大鹏),[1] C. Liu (刘晨),[1] Z. Q. Li (李志泉),[1] H. Jia (贾慧),[1] X. Q. Li (李湘庆),[3] C. Xu (徐川),[3] Z. H. Li (李智焕),[3] J. J. Sun (孙君杰),[3] L. H. Zhu (竺礼华),[6] P. Jones,[4] E. A. Lawrie,[4] J. J. Lawrie,[4] M. Wiedeking,[4] T. D. Bucher,[4,5] T. Dinoko,[4,7] L. Makhathini,[4,5] S. N. T. Majola,[4,8] S. P. Noncolela,[4,7] O. Shirinda,[4,5] J. Gál,[9] G. Kalinka,[9] J. Molnár,[9] B. M. Nyakó,[9] J. Timár,[9] K. Juhász,[10,‡] and M. Arogunjo[11]

[1]*Shandong Provincial Key Laboratory of Optical Astronomy and Solar-Terrestrial Environment, School of Space Science and Physics, Shandong University, Weihai 264209, People's Republic of China*

[2]*Shandong Agriculture And Engineering University, Jinan 250100, People's Republic of China*

[3]*School of Physics and State Key Laboratory of Nuclear Physics and Technology, Peking University, Beijing 100871, People's Republic of China*

[4]*iThemba LABS, National Research Foundation, P.O. Box: 722, Somerset West 7129, South Africa*

[5]*Department of Physics, University of Stellenbosch, Matieland 7602, South Africa*

[6]*School of Physics and Nuclear Energy Engineering, Beihang University, Beijing 100191, People's Republic of China*

[7]*Department of Physics, University of the Western Cape, P/B X17, Bellville 7535, South Africa*

[8]*Department of Physics, University of Cape Town, Rondebosch 7700, South Africa*

[9]*Institute for Nuclear Research, Hungarian Academy of Sciences, H-4001 Debrecen, Hungary*

[10]*Department of Information Technology, University of Debrecen, H-4010 Debrecen, Hungary*

[11]*Department of Physics, Federal University of Technology, Akure (FUTA) Ondo State, Nigeria*

(Received 5 October 2017; revised manuscript received 15 February 2018; published 10 April 2018)

Excited states in ^{155}Tm have been populated via the reaction ^{144}Sm(^{16}O, $p4n$)^{155}Tm at a beam energy of 118 MeV. The ground-state band has been extended and a new side band of the ground-state band is identified. E-GOS curves and potential energy surface calculations are employed to discuss the structure evolution of the ground-state band. The newly observed side band in ^{155}Tm is discussed based on the spin/energy systematics. In particular, the phenomenon of seniority inversion is proposed in ^{155}Tm, and a systematic study of this phenomenon in the $A \approx 150$ mass region is performed.

DOI: 10.1103/PhysRevC.97.044306

I. INTRODUCTION

Excited states in the light rare-earth nuclei near $A = 150$ have exhibited a wealth of interesting physics, such as shape coexistence [1–4], structure evolution [5–11], and seniority inversion [12–15]. The properties of the low-lying states in these nuclei were found to be sensitive to small changes in neutron number N [16]. The previous studies of the $N = 84$ nucleus ^{153}Tm have revealed that an interesting phenomenon of the seniority inversion exists, and single-particle excitation dominates the excitation spectra [13]. However, for the $N = 88$ nucleus ^{157}Tm, collective rotational excitation dominates the low-lying excitation spectra, and band termination was observed at high spin [17]. Therefore, the nucleus ^{155}Tm ($N = 86$) is a particularly good transitional nucleus located between single-particle and collective structures, which is suitable to investigate the structure evolution and seniority inversion.

Prior to this work, the $11/2^-$ ground state and the $1/2^+$ isomer in ^{155}Tm have been identified via the β decay of ^{155}Yb [18]. The low-lying experimental excitation spectra of ^{155}Tm were first reported in 1985 [19]. Two high-spin studies of ^{155}Tm were also reported in 2006 and 2007, respectively [20,21]. Although these two high-spin studies were in parallel, there exist some differences between them. In this paper, we report experimental results on the ground-state band of ^{155}Tm, together with a newly observed side band and the proposed seniority inverted state. The experimental procedure is described in Sec. II. Results and discussion are presented in Sec. III, and conclusions are given in Sec. IV.

II. EXPERIMENTAL PROCEDURE

Excited states in ^{155}Tm were populated via the ^{144}Sm(^{16}O, $p4n$)^{155}Tm fusion-evaporation reaction at a beam energy of 118 MeV. The beam was delivered by the Separated Sector Cyclotron (SSC) at iThemba LABS, South Africa. The target was 2.89 mg/cm^2 thick with a backing of 13.13 mg/cm^2 Pb. Deexcitation γ rays were detected using the AFRODITE array consisting of eight Compton-suppressed clover

*Corresponding author: sywang@sdu.edu.cn
†Corresponding author: mengj@pku.edu.cn
‡Deceased.

detectors [22]. Approximately 1.03×10^{10} γ-γ coincidence events were collected during the experiment. Energy and efficiency calibrations were performed with the standard ^{133}Ba and ^{152}Eu sources, which were mounted at the target position.

In order to extract the coincidence relationships between γ rays and the multipolarities of the transitions, the coincidence data were sorted off line into a symmetrized E_γ-E_γ matrix, an E_γ-E_γ-E_γ cube and two asymmetric angular distribution from oriented states (ADO) matrices. Two ADO matrices were constructed using the γ rays detected at all angles (y axis) against those detected at 135° and 90° (x axis), respectively. The experimental ADO ratio was calculated by $R_{\rm ADO}(\gamma) = I_\gamma(\text{at } 135°)/I_\gamma(\text{at } 90°)$, where the γ-ray intensities were determined in the coincidence spectra gated by the γ transitions (on the y axis) of any multipolarity. In the present geometry, by examining the known γ rays, the ADO ratios for stretched quadrupole and stretched pure dipole transitions were found to be about 1.2 and 0.8, respectively. The experimental results of the $5n$ exit channel (^{155}Yb) from the present experiment has been reported in Ref. [4].

TABLE I. γ-ray energies, relative intensities, spin-parity assignments, and measured ADO ratios for transitions shown in Fig. 1.

E_γ (keV)	I_γ	$I_i^\pi \rightarrow I_f^\pi$	ADO ratio
178.4	12.6(0.9)	$27/2^- \rightarrow 25/2^-$	0.99(0.17)
381.7	18.2(0.9)	$25/2^- \rightarrow 23/2^-$	0.93(0.10)
535.6	100.0	$15/2^- \rightarrow 11/2^-$	1.15(0.06)
560.1	49.5(1.9)	$27/2^- \rightarrow 23/2^-$	1.21(0.09)
596.5	89.8(2.9)	$19/2^- \rightarrow 15/2^-$	1.13(0.07)
619.9	77.6(2.7)	$23/2^- \rightarrow 19/2^-$	1.18(0.07)
658.7	6.2(0.6)	$(21/2^-) \rightarrow (17/2^-)$	1.18(0.11)
679.7	8.2(0.7)	$(25/2^-) \rightarrow (21/2^-)$	1.35(0.14)
718.2	~3	$43/2^- \rightarrow 39/2^-$	1.21(0.13)
718.7	~11	$31/2^- \rightarrow 27/2^-$	1.22(0.12)
738.4	10.1(0.5)	$35/2^- \rightarrow 31/2^-$	1.19(0.13)
760.6	5.5(0.4)	$39/2^- \rightarrow 35/2^-$	1.16(0.15)
826.0	<2.0	$(47/2^-) \rightarrow 43/2^-$	
844.6	6.3(0.4)	$(17/2^-) \rightarrow 15/2^-$	0.98(0.10)
906.8	2.4(0.2)	$(21/2^-) \rightarrow 19/2^-$	0.99(0.14)
966.6	2.1(0.2)	$(25/2^-) \rightarrow 23/2^-$	0.82(0.09)

III. RESULTS AND DISCUSSION

The partial level scheme of ^{155}Tm deduced from the present work is shown in Fig. 1. γ-ray energies, relative intensities, spin-parity assignments and measured ADO ratios for transitions shown in Fig. 1 are listed in Table I. The ground-state band (labeled band 1) has been extended up to spin $I^\pi = (47/2^-)$ by adding two new 718.2- and 826.0-keV transitions. Examples of background-subtracted γ-ray coincidence spectra are shown in Fig. 2. Most of the transitions in band 1 can be clearly seen from Figs. 2(a) and 2(b). The side band (labeled band 2), consisting of two $E2$ transitions, is a newly observed structure. In addition, three new linking transitions between bands 1 and 2 are also identified. The transitions in band 2 are visible in Fig. 2(b), together with the three linking transitions between bands 1 and 2.

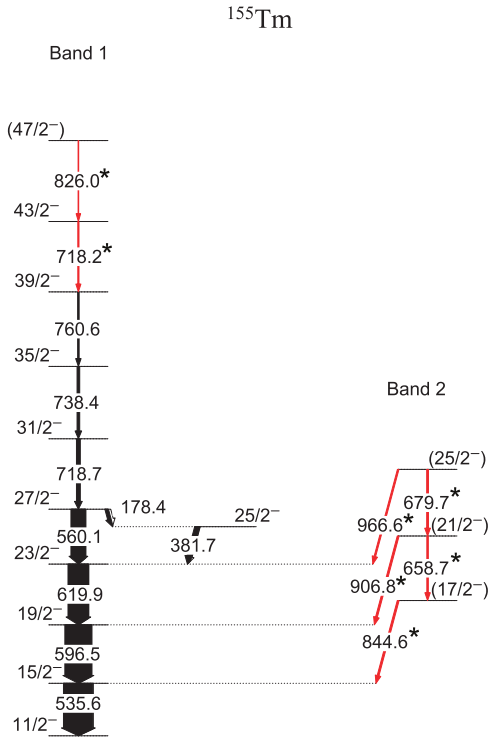

FIG. 1. Partial level scheme of ^{155}Tm deduced from the present work. Transition energies are given in keV, and the widths of the arrows represent the relative intensities of the γ transitions. The newly observed transitions are indicated by asterisks and red lines.

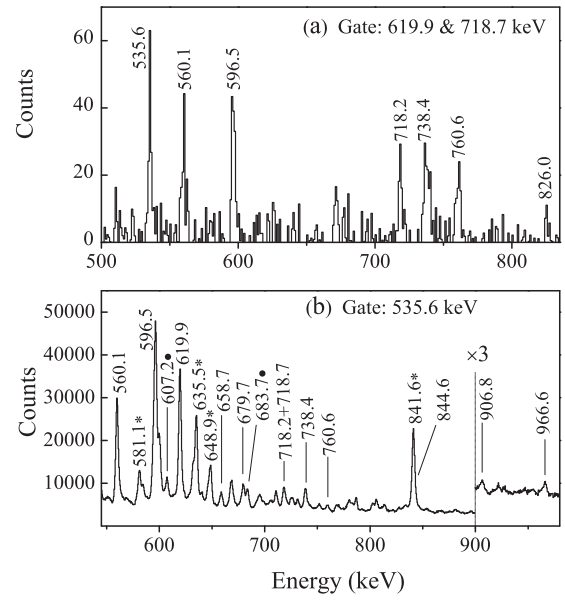

FIG. 2. Examples of gated coincidence spectra: (a) Spectrum double gated by the 619.9- and 718.7-keV transitions of band 1. (b) Spectrum gated by the 535.6-keV transition. The peaks marked with asterisks are transitions depopulating the multiparticle states of ^{155}Tm, which are not included in Fig. 1. The contaminant peaks from ^{156}Yb have been marked with filled circles.

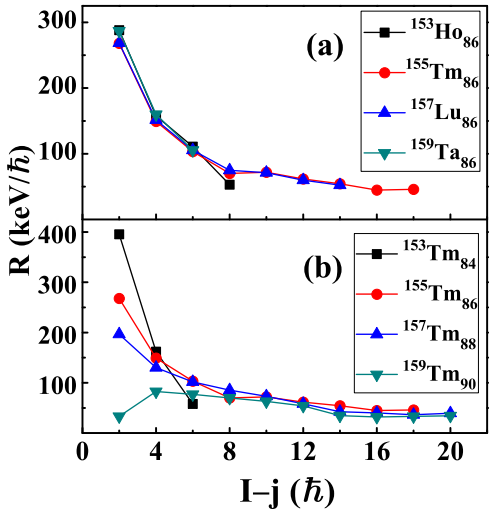

FIG. 3. (a) E-GOS curves for the $N = 86$ odd-A isotones, (b) E-GOS curves for the $Z = 69$ odd-A isotopes. Data are taken from Refs. [13,14,17,31–35] and the present work for ^{155}Tm.

It should be noted that, for the partial level scheme of ^{155}Tm shown in Fig. 1, there exist two differences between Ref. [20] and Ref. [21]. The first difference is the spin-parity assignments of the level that depopulates via the 381.7-keV transition, Ref. [20] assigned this level as $I^{\pi} = 25/2^{-}$, while Ref. [21] suggested $I^{\pi} = (23/2^{-},27/2^{-})$ for this level. The present measured ADO ratios for the 381.7- and 178.4-keV transitions are 0.93(0.10) and 0.99(0.17), respectively. These indicate that both of the two transitions are of mixed $M1/E2$ character. Therefore, the level that depopulates via the 381.7-keV transition has been assigned $I^{\pi} = 25/2^{-}$, which is consistent with the corresponding assignment of Ref. [20]. The other difference is that the energies of the transition, which feeds the $31/2^{-}$ state are 730 keV [20] and 739 keV [21], respectively. As seen in Fig. 2(a), the 738.4-keV transition is clearly visible, while the 730-keV transition is not visible. Therefore, the energy of the transition, which feeds the $31/2^{-}$ state is 738.4 keV.

A. Band 1

The energy spacings of the low-lying states of band 1 are almost equal, and are similar to those of the neighboring $N = 86$ even-even ^{154}Er [23] and ^{156}Yb [24] nuclei. The low-lying states of these two nuclei have been suggested to show vibrational character. As shown in Fig. 1, the energy spacings gradually increase above the $27/2^{-}$ state, implying the possible character of a rotor. In this regard, band 1 in ^{155}Tm could have a transition from quasivibrational to quasirotational structure with increasing spin.

To highlight the character of band 1, we employ the E-GOS (E_{γ} over spin) prescription [25]. This prescription has been widely used to distinguish vibrational and rotational modes as a function of spin in the even-even transitional nuclei [25–30]. For the odd-A nuclei, a weak-coupling approximation was used, and the E-GOS ratio was assumed to be $R = \frac{E_{\gamma}(I \to I-2)}{I-j}$, where I is the level spin and j is the spin of the band head [26]. Figure 3 shows the systematic comparison of E-GOS curves

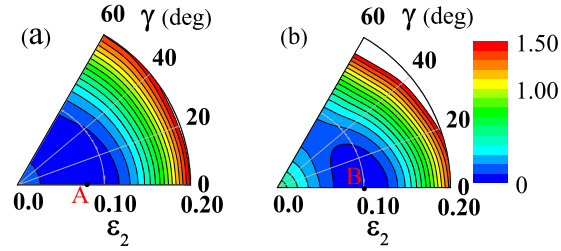

FIG. 4. Potential energy surfaces of ^{155}Tm as a function of the quadrupole deformation ε_2 and the triaxial deformation γ at $\hbar\omega = 0.0$ MeV for the quasiparticle configuration (a) $\pi h_{11/2}$, (b) $\pi h_{11/2} \otimes \nu f_{7/2} h_{9/2}$. The distance between the contour lines is 100 keV.

for the odd-A isotopes of Tm and odd-A $N = 86$ isotones. As shown in Fig. 3(a), the E-GOS curves of available data in the odd-A, $N = 86$ isotones are very similar, which indicates that the level structures in these isotones are almost independent of the proton number. In contrast to Fig. 3(a), the E-GOS curves for the Tm isotopes in Fig. 3(b) exhibit the different systematic features. Previous studies suggested that ^{153}Tm [13] and ^{157,159}Tm [17,34] own single-particle and rotational characters, respectively. As can be seen in Fig. 3(b), for the low-lying region, the R values of ^{155}Tm are situated between ^{153}Tm and ^{157,159}Tm. As the spin increases, the R values of ^{155}Tm are very close to ^{157,159}Tm. Hence, the evolution from quasivibrational to quasirotational modes in the band 1 of ^{155}Tm is proposed based on the systematic comparison of E-GOS curves.

To get further insight into the property of the ground-state band, the potential energy surface calculations [36,37] have been performed. It is based on the hybrid potential combining a spherical Woods-Saxon potential with a deformed Nilsson potential [37]. Pairing has been taken into account by using values of $\Delta_p = 1.16$ MeV, $\Delta_n = 0.97$ MeV. The calculated potential energy surfaces for the one-quasiparticle $\pi h_{11/2}$ configuration and the three-quasiparticle $\pi h_{11/2} \nu f_{7/2} h_{9/2}$ configuration involving neutron excitations, are illustrated as a function of the deformation parameters (ε_2, γ) in Figs. 4(a) and 4(b), respectively. The $\pi h_{11/2}$ configuration represents the ground state in ^{155}Tm, and the fully aligned $\pi h_{11/2} \nu f_{7/2} h_{9/2}$ configuration corresponds to the yrast $27/2^{-}$ state in ^{155}Tm based on weak coupling of the unpaired $h_{11/2}$ proton to the yrast 8^{+} state ($\nu f_{7/2} h_{9/2}$ configuration) in ^{154}Er [38]. As shown in Fig. 4, the energy minima for $\pi h_{11/2}$ and $\pi h_{11/2} \nu f_{7/2} h_{9/2}$ configurations appear at A($\varepsilon_2 = 0.08$, $\gamma = 0^{\circ}$) and B($\varepsilon_2 = 0.10$, $\gamma = 0^{\circ}$), respectively. Figure 4(a) shows that the ground-state shape of ^{155}Tm is rather soft, inducing the formation of a vibrational structure, which is consistent with the low-lying vibrational spectra observed in the present experiment. Compared with Fig. 4(a), the quadrupole deformation ε_2 of energy minimum exhibited in Fig. 4(b) becomes larger. In addition, the potential energy surface of the $\pi h_{11/2} \nu f_{7/2} h_{9/2}$ configuration becomes stiffer compared to that of the $\pi h_{11/2}$ configuration. This indicates that the shape of ^{155}Tm is slightly stabilized when an $f_{7/2}$ neutron is excited to the $h_{9/2}$ orbital, which is consistent with the experimental excitation spectra above the yrast $27/2^{-}$ state. Thus, the present calculations further support the interpretation of the evolution from quasivibrational to

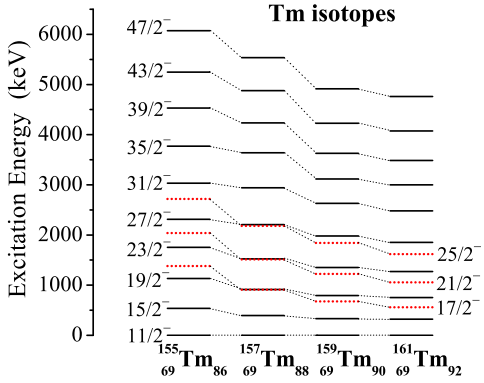

FIG. 5. Comparison of levels in bands 1 and 2 of ^{155}Tm with those in the heavier odd-A Tm isotopes. The levels in bands 1 and 2 of ^{155}Tm are denoted by the solid lines and red dotted lines, respectively. The corresponding levels in the heavier odd-A Tm isotopes are connected to guide the eye. Data are taken from Refs. [17,34,39] and the present work for ^{155}Tm.

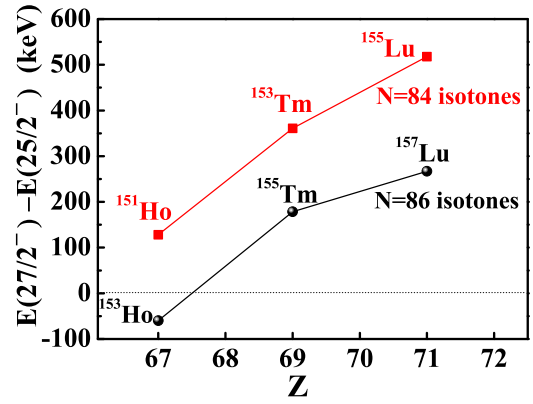

FIG. 6. Systematics for the energy differences between the yrast $27/2^-$ and $25/2^-$ states in the $N = 84$ and $N = 86$ odd-A isotones. Data are taken from Refs. [12–15,31,32] and the present work.

quasirotational structure for the ground-state band in ^{155}Tm, and this evolution can be ascribed to neutron excitation.

B. Newly identified side band

Band 2 is a newly identified side band. Similar structures have been observed in the heavier odd-A Tm isotopes. To understand the possible excitation mechanism of this band, a systematic comparison of bands 1 and 2 with those corresponding states in the odd-A Tm isotopes was made in Fig. 5. As shown in Fig. 5, the excitation energies of the states exhibit a good systematic feature from ^{155}Tm to ^{161}Tm. The similar structure in $^{157-161}$Tm has been assigned as signature $\alpha = \frac{1}{2}$ decay sequence based on the $\pi h_{11/2}$ state. Therefore, band 2 in ^{155}Tm may be associated with $\alpha = \frac{1}{2}$ sequence of the $\pi h_{11/2}$ state based on the systematics.

C. Yrast $27/2^-$ to $25/2^-$ energy anomaly

A particular interesting aspect in the present work is the existence of the yrast $27/2^-$ to $25/2^-$ energy anomaly in the $N = 86$ nucleus ^{155}Tm. In general, the number of unpaired nucleons increases monotonically towards higher excitation energy along the yrast line. If this rule is violated, energy anomaly occurs. This phenomenon has been observed in the $N = 84$ isotones ^{151}Ho, ^{153}Tm, and ^{155}Lu, which is called seniority (the number of unpaired nucleons) inversion [12–15].

In the next step we focus on the yrast $25/2^-$ and $27/2^-$ states in ^{155}Tm. Based on the comparison with neighboring nuclei and weak coupling, the yrast $25/2^-$ and $27/2^-$ states in ^{155}Tm can be interpreted as the $\pi h^3_{11/2}\nu f_{7/2}h_{9/2}$ and $\pi h_{11/2}\nu f_{7/2}h_{9/2}$ configurations, respectively. Based on these configurations, the seniority quantum numbers of the $25/2^-$ and $27/2^-$ states are 5 and 3, respectively. As shown in Fig. 1, the $25/2^-$ state lies lower in energy than the $27/2^-$ state, thereby the energy anomaly occurs in ^{155}Tm. For the $(\pi h^3_{11/2}\nu f_{7/2}h_{9/2})_{25/2^-}$ state, the three protons respectively occupy the $m = +11/2$, $+9/2$ and $-11/2$ substates, thus the $(\pi h_{11/2}\nu h_{9/2})_{1^+}$ coupling becomes dominant [12,13]. This attractive $(\pi h_{11/2}\nu h_{9/2})_{1^+}$ interaction lowers the $(\pi h^3_{11/2}\nu f_{7/2}h_{9/2})_{25/2^-}$ state with respect to the $(\pi h_{11/2}\nu f_{7/2}h_{9/2})_{27/2^-}$ state, leading to the yrast $27/2^-$ to $25/2^-$ energy anomaly.

To better understand the character of the energy anomaly in this region, a systematic study of yrast $27/2^-$ to $25/2^-$ energy anomaly is performed. It is worth mentioning that the energy anomaly probably exists in ^{157}Lu based on the experimental excitation spectra [14], for the completeness of systematics, the corresponding data of ^{157}Lu [14] and ^{153}Ho [31] are also included. Systematics for the energy differences between the yrast $27/2^-$ and $25/2^-$ states in the $N = 84$ and $N = 86$ odd-A isotones are shown in Fig. 6. The inversion energies ($E_{27/2^-} - E_{25/2^-}$) of the $N = 84$ and $N = 86$ isotones gradually increase by ~200 keV as the proton number increases, which implies that the $(\pi h_{11/2}\nu h_{9/2})_{1^+}$ attractive interaction increases by ~200 keV when one more pair of protons occupy the $\pi h_{11/2}$ orbital. In contrast, as the neutron number increases from 84 to 86, the inversion energies of Ho, Tm, and Lu isotopes all decrease by ~200 keV, indicating that the $(\pi h_{11/2}\nu h_{9/2})_{1^+}$ attractive interaction decreases by ~200 keV when one more pair of neutrons occupy the $\nu f_{7/2}$ orbital. Furthermore, it should be noted that the lines corresponding to the $N = 84$ and $N = 86$ odd-A isotones are almost in parallel in Fig. 6, indicating that the $(\pi h_{11/2}\nu h_{9/2})_{1^+}$ interaction for the $N = 84$ and $N = 86$ isotones increases by similar amplitude as the proton number increases, which further supports the yrast $27/2^-$ to $25/2^-$ energy anomaly in $N = 86$ nucleus ^{155}Tm.

Based on the systematic trend shown in Fig. 6, the energy anomaly is expected to occur in ^{157,159}Ta, and the inversion energies of Ta ($Z = 73$) isotopes should be larger. Further experimental investigations are highly encouraged to be performed to confirm this hypothesis.

IV. CONCLUSION

Excited states in ^{155}Tm have been investigated by in-beam spectroscopy using the ^{144}Sm(^{16}O, $p4n$)^{155}Tm fusion-evaporation reaction at a beam energy of 118 MeV. The ground-state band has been extended by adding two new transitions and one side band is established for the first time. The systematic comparisons of the E-GOS curves indicate that an evolution from quasivibrational to quasirotational structure for the ground-state band occurs. The calculated potential

energy surfaces suggest that the neutron excitation induces the vibration-rotation evolution. Based on systematics, the newly identified band 2 may be associated with $\alpha = \frac{1}{2}$ sequence based on the $\pi h_{11/2}$ state. A seniority inversion is proposed to exist in ^{155}Tm and a systematic study of this phenomenon in the $A \approx 150$ mass region is performed, reflecting that the $(\pi h_{11/2} \nu h_{9/2})_{1^+}$ strong attractive interaction plays an essential role in the phenomenon of the seniority inversion.

ACKNOWLEDGMENTS

This work is partly supported by the Natural Science Foundation (Grants No. 11622540, No. 11647012, No. 11405096, No. 11675094, No. 11235001, and No. 11320101004), and the Shandong Natural Science Foundation (Grant No. ZR2014AQ012) of China. The computations were carried out on an HP Proliant DL785G6 server hosted by the Institute of Space Science of Shandong University.

[1] B. M. Nyakó, J. Simpson, P. J. Twin, D. Howe, P. D. Forsyth, and J. F. Sharpey-Schafer, Phys. Rev. Lett. **56**, 2680 (1986).
[2] M. B. Smith, D. E. Appelbe, P. J. Twin, C. W. Beausang, F. A. Beck, M. A. Bentley, D. M. Cullen, D. Curien, P. J. Dagnall, G. deFrance, G. Duchene, S. Erturk, C. Finck, B. Haas, I. M. Hibbert, J. C. Lisle, B. M. Nyako, C. D. OLeary, C. Rigollet, H. Savajols, J. Simpson, O. Stezowski, J. Styczen, J. P. Vivien, and K. Zuber, Phys. Rev. C **61**, 034314 (2000).
[3] D. E. Appelbe, P. J. Twin, C. W. Beausang, D. M. Cullen, D. Curien, G. Duchene, S. Erturk, C. Finck, B. Haas, E. S. Paul, D. C. Radford, C. Rigollet, M. B. Smith, O. Stezowski, J. C. Waddington, and A. N. Wilson, Phys. Rev. C **66**, 044305 (2002).
[4] X. Q. Li *et al.*, Phys. Rev. C **94**, 024337 (2016).
[5] F. S. Stephens, M. A. Deleplanque, R. M. Diamond, A. O. Macchiavelli, and J. E. Draper, Phys. Rev. Lett. **54**, 2584 (1985).
[6] E. S. Paul, S. V. Rigby, M. A. Riley, J. Simpson, D. E. Appelbe, D. B. Campbell, P.T.W. Choy, R. M. Clark, M. Cromaz, A. O. Evans, P. Fallon, A. Gorgen, D. T. Joss, I. Y. Lee, A. O. Macchiavelli, P. J. Nolan, A. Pipidis, D. Ward, and I. Ragnarsson, Phys. Rev. C **79**, 044324 (2009).
[7] E. S. Paul, P. J. Twin, A. O. Evans, A. Pipidis, M. A. Riley, J. Simpson, D. E. Appelbe, D. B. Campbell, P.T.W. Choy, R. M. Clark, M. Cromaz, P. Fallon, A. Gorgen, D. T. Joss, I. Y. Lee, A. O. Macchiavelli, P. J. Nolan, D. Ward, and I. Ragnarsson, Phys. Rev. Lett. **98**, 012501 (2007).
[8] Z. Y. Li, H. Hua, S. Y. Wang, J. Meng, Z. H. Li, X. Q. Li, F. R. Xu, H. L. Liu, S. Q. Zhang, Y. L. Ye, D. X. Jiang, T. Zheng, L. Y. Ma, F. Lu, F. Y. Fan, L. Y. Han, H. Wang, J. Xiao, D. Chen, X. Fang, J. L. Lou, S. G. Zhou, L. H. Zhu, X. G. Wu, G. S. Li, C. Y. He, Y. Liu, X. Q. Li, X. Hao, B. Pan, and L. H. Li, Phys. Rev. C **77**, 064323 (2008).
[9] Y. Zheng *et al.*, Eur. Phys. J. A **14**, 133 (2002).
[10] C. Xu, H. Hua, X. Q. Li, J. Meng, Z. H. Li, F. R. Xu, Y. Shi, H. L. Liu, S. Q. Zhang, Z. Y. Li, L. H. Zhu, X. G. Wu, G. S. Li, C. Y. He, S. G. Zhou, S. Y. Wang, Y. L. Ye, D. X. Jiang, T. Zheng, J. L. Lou, L. Y. Ma, E. H. Wang, Y. Y. Cheng, and C. He, Phys. Rev. C **83**, 014318 (2011).
[11] C. Xu, H. Hua, X. Q. Li, S. Q. Zhang, J. Meng, Z. H. Li, F. R. Xu, Y. Y. Cheng, C. He, J. J. Sun, Y. Shi, H. L. Liu, Z. Y. Li, L. H. Zhu, X. G. Wu, G. S. Li, C. Y. He, Y. Zheng, S. G. Zhou, S. Y. Wang, Y. L. Ye, D. X. Jiang, T. Zheng, J. L. Lou, L. Y. Ma, E. H. Wang, L. L. Wang, and B. Zhang, Phys. Rev. C **87**, 034325 (2013).
[12] C. T. Zhang, P. Kleinheinz, M. Piiparinen, R. Collatz, T. Lönnroth, G. Sletten, and J. Blomqvist, Z. Phys. A **348**, 65 (1994).
[13] C. T. Zhang, P. Kleinheinz, M. Piiparinen, R. Collatz, T. Lönnroth, G. Sletten, and J. Blomqvist, Z. Phys. A **348**, 249 (1994).
[14] K. Y. Ding, J. A. Cizewski, D. Seweryniak, H. Amro, M. P. Carpenter, C. N. Davids, N. Fotiades, R.V.F. Janssens, T. Lauritsen, C. J. Lister, D. Nisius, P. Reiter, J. Uusitalo, I. Wiedenhover, and A. O. Macchiavelli, Phys. Rev. C **64**, 034315 (2001).
[15] R. J. Carroll, B. Hadinia, C. Qi, D. T. Joss, R. D. Page, J. Uusitalo, K. Andgren, B. Cederwall, I. G. Darby, S. Eeckhaudt, T. Grahn, C. Gray-Jones, P. T. Greenlees, P. M. Jones, R. Julin, S. Juutinen, M. Leino, A. P. Leppanen, M. Nyman, J. Pakarinen, P. Rahkila, M. Sandzelius, J. Saren, C. Scholey, D. Seweryniak, and J. Simpson, Phys. Rev. C **94**, 064311 (2016).
[16] R. F. Casten, D. D. Warner, D. S. Brenner, and R. L. Gill, Phys. Rev. Lett. **47**, 1433 (1981).
[17] M. A. Riley, T. B. Brown, N. R. Johnson, Y. A. Akovali, C. Baktash, M. L. Halbert, D. C. Hensley, I. Y. Lee, F. K. McGowan, A. Virtanen, M. E. Whitley, J. Simpson, L. Chaturvedi, L. H. Courtney, V. P. Janzen, L. L. Riedinger, and T. Bengtsson, Phys. Rev. C **51**, 1234 (1995).
[18] K. S. Toth, K. S. Vierinen, M. O. Kortelahti, D. C. Sousa, J. M. Nitschke, and P. A. Wilmarth, Phys. Rev. C **44**, 1868 (1991).
[19] R. Kossakowski, J. Jastrzebski, P. Rymuza, W. Skulski, A. Gizon, S. André, J. Genevey, J. Gizon, and V. Barci, Phys. Rev. C **32**, 1612 (1985).
[20] Y. Liu *et al.*, High Energy Phys. and Nucl. Phys. **30**, 160 (2006).
[21] R. Raut *et al.*, Nucl. Phys. A **794**, 1 (2007).
[22] R. A. Bark, M. Lipoglavšek, S. M. Maliage, S. S. Ntshangase, and A. Shevchenko, J. Phys. G **31**, S1747 (2005).
[23] C. Baktash, E. der Mateosian, O. C. Kistner, and A. W. Sunyar, Phys. Rev. Lett. **42**, 637 (1979).
[24] C. J. Lister, D. Horn, C. Baktash, E. der Mateosian, O. C. Kistner, and A. W. Sunyar, Phys. Rev. C **23**, 2078 (1981).
[25] P. H. Regan, C. W. Beausang, N. V. Zamfir, R. F. Casten, J. Y. Zhang, A. D. Yamamoto, M. A. Caprio, G. Gurdal, A. A. Hecht, C. Hutter, R. Krucken, S. D. Langdown, D. A. Meyer, and J. J. Ressler, Phys. Rev. Lett. **90**, 152502 (2003).
[26] P. H. Regan *et al.* in *The Frontiers of Nuclear Structure*, edited by P. Fallon and R. Clark, AIP Conf. Proc. No. 656 (AIP, Melville, 2003), p. 422.
[27] R. B. Cakirli, R. F. Casten, E. A. McCutchan, H. Ai, H. Amro, M. Babilon, C. W. Beausang, A. Heinz, R. O. Hughes, D. A. Meyer, C. Plettner, J. J. Ressler, and N. V. Zamfir, Phys. Rev. C **70**, 044312 (2004).
[28] D. Sohler, J. Timar, G. Rainovski, P. Joshi, K. Starosta, D. B. Fossan, J. Molnar, R. Wadsworth, A. Algora, P. Bednarczyk, D. Curien, Z. Dombradi, G. Duchene, A. Gizon, J. Gizon, D. G. Jenkins, T. Koike, A. Krasznahorkay, E. S. Paul, P. M. Raddon, J. N. Scheurer, A. J. Simons, C. Vaman, A. R. Wilkinson, and L. Zolnai, Phys. Rev. C **71**, 064302 (2005).

[29] H. G. Börner, R. F. Casten, M. Jentschel, P. Mutti, W. Urban, and N. V. Zamfir, Phys. Rev. C **84**, 044326 (2011).
[30] G. S. Li, M. L. Liu, X. H. Zhou, Y. H. Zhang, Y. X. Liu, N. T. Zhang, W. Hua, Y. Zheng, Y. D. Fang, S. Guo, J. G. Wang, Y. H. Qiang, B. Ding, L. Ma, M. Oshima, Y. Toh, M. Koizumi, A. Osa, Y. Hatsukawa, and M. Sugawara, Phys. Rev. C **89**, 054303 (2014).
[31] D. C. Radford *et al.*, Phys. Lett. B **126**, 24 (1983).
[32] D. Pramanik *et al.*, Phys. Rev. C **94**, 024311 (2016).
[33] A. Keenan, R. D. Page, J. Simpson, N. Amzal, J. F. C. Cocks, D. M. Cullen, P. T. Greenlees, S. L. King, K. Helariutta, P. Jones, D. T. Joss, R. Julin, S. Juutinen, H. Kankaanpaa, P. Kuusiniemi, M. Leino, M. Muikku, A. Savelius, M. B. Smith, and M. J. Taylor, Phys. Rev. C **63**, 064309 (2001).
[34] J. Gascon, P. Taras, D. C. Radford, D. Ward, H. R. Andrews, and F. Banville, Nucl. Phys. A **467**, 539 (1987).
[35] C. W. Reich, Nucl. Data Sheets **113**, 157 (2012).
[36] S. Frauendorf, Nucl. Phys. A **557**, 259c (1993).
[37] V. I. Dimitrov, F. Dönau, and S. Frauendorf, Phys. Rev. C **62**, 024315 (2000).
[38] C. Schück, M. A. Deleplanque, R. M. Diamond, F. S. Stephens, and J. Dudek, Nucl. Phys. A **496**, 385 (1989).
[39] S. J. Warburton *et al.*, Nucl. Phys. A **591**, 323 (1995).